Mono- and Bis(silyl) Complexes of Molybdenum and Tungsten. Synthesis, Structures, and ^{29}Si NMR Trends

Timothy S. Koloski, Doris C. Pestana, Patrick J. Carroll, and Donald H. Berry*[,1]

Department of Chemistry and Laboratory for Research on the Structure of Matter, University of Pennsylvania, Philadelphia, Pennsylvania 19104-6323

Received October 5, 1993[⊛]

The photochemical reaction (350 nm) of the group 6 metallocene dihydrides Cp_2MH_2 (M = Mo, W) with hydridosilanes, $HSiR_3$, produces good to excellent yields of the corresponding silyl hydride complexes, $Cp_2M(H)(SiR_3)$ (M = Mo: SiR_3 = $SiMe_2H$, **3**; $SiMe_2Cl$, **4a**; $SiMe_3$, **5a**; Si(*t*-Bu)$_2$H, **6a**; Si(*t*-Bu)$_2$Cl, **7**; M = W: SiR_3 = $SiMe_2Cl$, **8**; $SiMe_3$, **9**). Methylcyclopentadienyl derivatives $Cp'_2Mo(H)(SiR_3)$ (SiR_3 = $SiMe_3$, **5b**; SiR_3 = Si(*t*-Bu)$_2$H, **6b**) have also been prepared. Chlorination of the metal hydride in **4a** yields $Cp_2Mo(Cl)(SiMe_2Cl)$, **4b**. Bis(silyl) complexes $Cp_2W(SiMe_3)(SiR_3)$ (SiR_3 = $SiMe_3$, **11**; $SiMe_2Cl$, **12**; Si(*i*-Pr)$_2$Cl, **13**; Si(*t*-Bu)$_2$H, **14**) are synthesized in excellent yields from the reaction of the stable silene complex $Cp_2W(\eta^2\text{-}SiMe_2{=}CH_2)$ with the corresponding hydridosilanes. The molybdenum complexes **3**, **4a**, **5b**, and **6b** and the tungsten complexes **9**, **13**, and **14** have been structurally characterized by single crystal X-ray diffraction studies. The observed metal–silicon bond lengths generally correlate with steric congestion, with the exception of the chlorosilyl derivatives which exhibit quite short M–Si distances and extremely long Si–Cl distances. The anomalous features of the chlorosilyl complexes are attributed to both inductive effects and π-back-bonding from the metal into the Si–Cl σ^* orbital, which leads to some degree of silylene character. Trends in the ^{29}Si NMR parameters, in particular the tungsten–silicon coupling constants ($^1J_{W-Si}$), provide further evidence for partial silylene character in the chlorosilyl derivatives. Complexes containing the bulky Si(*t*-Bu)$_2$H ligand exhibit hindered rotation around the M–Si bond in solution as determined by variable temperature ^{1}H NMR. Barriers to rotation of the silyl group are 20.7 ± 0.6 kcal mol^{-1} in **6a**, 20.6 ± 0.5 kcal mol^{-1} in **6b**, and 13.5 ± 0.1 kcal mol^{-1} in **14**.

Introduction

In recent reports we have described the synthesis of disilene ($Me_2Si{=}SiMe_2$)[2] and silene ($Me_2Si{=}CH_2$)[3] complexes of group 6 metallocenes, which are among the first examples of stable metal complexes of unsaturated silicon ligands.[4-7] Analysis of the unusual structural and spectroscopic properties of these novel silaolefin complexes has been complicated, however, by the paucity of known tungsten and molybdenum silyl compounds for comparison. In this contribution we describe general syntheses and molecular structures of molybdenum and tungsten metallocenes containing one and two silyl groups. In addition, trends in the ^{29}Si NMR parameters are reported and analyzed in terms of structural and electronic features of the complexes.

When applicable, the oxidative addition of hydridosilanes (R_3SiH) to coordinatively unsaturated metal complexes is the most convenient route to transition metal silyls because of the ready availability and low cost of hydridosilane starting materials.[8,9] Previous work from this laboratory has shown that oxidation addition of silanes to photochemically generated unsaturated tantalum complexes is a high-yield route to a wide range of mono- and bis(silyl) tantalum complexes.[10] Green and co-workers have shown in extensive studies that many tungsten and molybdenum derivatives can be prepared by oxidative addition of σ-bonds to metallocenes generated photochemically from the dihydrides, Cp_2MH_2.[11] The synthesis of $Cp_2W(H)(SiCl_3)$ in <50% yield by the thermolysis of Cp_2WH_2 in the presence of a large excess of trichlorosilane has been previously reported by Cardoso, Clark, and

---

[⊛] Abstract published in *Advance ACS Abstracts,* December 15, 1993.

[1] Alfred P. Sloan Fellow, 1990–1994.

[2] (a) Berry, D. H.; Chey, J. C.; Zipin, H. S.; Carroll, P. J. *J. Am. Chem. Soc.* **1990**, *112*, 452. (b) Berry, D. H.; Chey, J. C.; Zipin, H. S.; Carroll, P. J. *Polyhedron* **1991**, *10*, 1189. (c) Hong, P.; Damrauer, N. H.; Carroll, P. J.; Berry, D. H. *Organometallics* **1993**, *12*, 3698.

[3] (a) Koloski, T. S.; Carroll, P. J.; Berry, D. H. *J. Am. Chem. Soc.* **1990**, *112*, 6405. (b) Koloski, T. S., Ph.D. Thesis, 1991, University of Pennsylvania.

[4] (a) Campion, B. K.; Heyn, R.; Tilley, T. D. *J. Am. Chem. Soc.* **1988**, *110*, 7558. (b) Campion, B. K.; Heyn, R.; Tilley, T. D. *J. Am. Chem. Soc.* **1990**, *112*, 4079. (c) Campion, B. K.; Heyn, R.; Tilley, T. D. Rheingold, A. L. *J. Am. Chem. Soc.* **1993**, *115*, 5527.

[5] (a) Pham, E. K.; West, R. *J. Am. Chem. Soc.* **1989**, *111*, 7667. (b) Pham, E. K.; West, R. *Organometallics* **1990**, *9*, 1517.

[6] (a) Procopio, L. J.; Carroll, P. J.; Berry, D. H. *J. Am. Chem. Soc.* **1991**, *113*, 1870. (b) Procopio, L. J.; Carroll, P. J.; Berry, D. H. *Organometallics* **1993**, *12*, 3087.

[7] Ando, W.; Yamamoto, T.; Saso, H.; Kabe, Y. *J. Am. Chem. Soc.* **1991**, *113*, 2791.

[8] Chalk, A. J.; Harrod, J. F. *J. Am. Chem. Soc.* **1965**, *87*, 16.

[9] For reviews of metal–silicon compounds, see: (a) Tilley, T. D. In *The Chemistry of Organic Silicon Compounds*; Patai, S., Rappoport, Z., Eds.; Wiley: New York, 1989; Vol. 2, p 1415. (b) Tilley, T. D. In *The Silicon–Heteroatom Bond*; Patai, S., Rappoport, Z., Eds.; Wiley: New York, 1991; Chapters 9 and 10. (c) MacKay, K. M.; Nicholson, B. K. In *Comprehensive Organometallic Chemistry*; Wilkinson, G., Stone, F. G. A., Abel, E., Eds.; Pergamon: London, 1982; Vol. 4, p 1043. (d) Aylett, B. J. *Adv. Inorg. Chem. Radiochem.* **1982**, *25*, 1.

[10] Jiang, Q.; Carrol, P. J.; Berry, D. H. *Organometallics* **1991**, *10*, 3648.

[11] (a) Grebenik, P. D.; Green, M. L. H.; Kelland, M. A.; Leach, J. B.; Mountford, P. *J. Chem. Soc., Chem. Commun.* **1989**, 1397. (b) Grebenik, P. D.; Green, M. L. H.; Kelland, M. A.; Leach, J. B.; Mountford, P.; Stringer, G.; Walker, N. M.; Wong, L. L. *J. Chem. Soc., Chem. Commun.* **1988**, 799. (c) Grebenik, P. D.; Green, M. L. H.; Izquierdo, A.; Mtetwa, V. S. B.; Prout, K. *J. Chem. Soc., Dalton Trans.* **1987**, 9. (d) Grebenik, P. D.; Green, M. L. H.; Izquierdo, A. *J. Chem. Soc., Chem. Commun.* **1981**, 186. (e) Berry, M.; Elmitt, K.; Green, M. L. H. *J. Chem. Soc., Dalton Trans.* **1979**, 1950. (f) Berry, M.; Davies, S. G.; Green, M. L. H. *J. Chem. Soc., Chem. Commun.* **1978**, 99. (g) Farrugia, L.; Green, M. L. H. *J. Chem. Soc., Chem. Commun.* **1975**, 416. (h) Elmitt, K.; Green, M. L. H.; Forder, R. A.; Jefferson, I.; Prout, K. *J. Chem. Soc., Chem. Commun.* **1974**, 747. (i) Giannotti, C.; Green, M. L. H. *J. Chem. Soc., Chem. Commun.* **1972**, 1114.

0276-7333/94/2313-0489$04.50/0

Table 1. ^{1}H and ^{13}C NMR Data for Molybdenum and Tungsten Silyl Complexes

no.	compound	^{1}H^a	^{13}C{^{1}H}^{a}
3	$Cp_2Mo(H)(SiMe_2H)$	4.80 (sept, $^3J_{H-H}$ = 3.8, 1H, SiH), 4.12 (s, 10H, Cp), 0.53 (d, $^3J_{H-H}$ = 3.8, 1H, $SiMe_2$), −7.93 (s, br, 1H, MoH)	77.8 (Cp), 5.4 ($SiMe_2$)
4a	$Cp_2Mo(H)(SiMe_2Cl)$	4.20 (s, 10H, Cp), 0.79 (s, 6H, $SiMe_2$) −8.18 (s, 1H, MoH)	79.5 (Cp), 14.4 ($SiMe_2$)
4b	$Cp_2Mo(Cl)(SiMe_2Cl)$	4.38 (s, 10H, Cp), 0.99 (s, 6H, $SiMe_2$)	91.0 (Cp), 9.7 ($SiMe_2$)
5a	$Cp_2Mo(H)(SiMe_3)$	4.11 (s, 10H, Cp), 0.41 (s, 9H, $SiMe_3$) −7.62 (s, 1H, MoH)	77.4 (Cp), 9.7 ($SiMe_3$)
5b	$Cp'_2Mo(H)(SiMe_3)$	4.23 (br, 2H, $MeC_5\mathit{H}_4$), 4.05 (br, 2H, $MeC_5\mathit{H}_4$), 3.98 (br, 2H, $MeC_5\mathit{H}_4$), 3.85 (br, 2H, $MeC_5\mathit{H}_4$), 1.66 (s, 6H, $\mathit{Me}C_5H_4$), 0.47 (s, 9H, $SiMe_3$), −7.52 (s, 1H, MoH)	94.0 ($Me\mathit{C}_5H_4$), 83.0 ($Me\mathit{C}_5H_4$), 81.3 ($Me\mathit{C}_5H_4$), 77.9 ($Me\mathit{C}_5H_4$), 76.9 ($Me\mathit{C}_5H_4$), 15.2 ($\mathit{Me}C_5H_4$), 10.0 ($SiMe_3$)
6a	$Cp_2Mo(H)(Si(\mathit{t}\text{-}Bu)_2H)$	4.24 (s, 5H, Cp), 4.21 (s, 5H, Cp), 4.00 (s, 1H, SiH), 1.36 (s, 9H, CMe_3), 1.23 (s, 9H, CMe_3), −7.93 (s, 1H, MoH)	79.5 (Cp), 75.5 (Cp), 33.9 ($C(\mathit{Me})_3$), 33.4 ($C(\mathit{Me})_3$), 27.2 ($\mathit{C}(Me)_3$), 26.5 ($\mathit{C}(Me)_3$)
6b	$Cp'_2Mo(H)(Si(\mathit{t}\text{-}Bu)_2H)$	4.78 (br, 1H, $MeC_5\mathit{H}_4$), 4.39 (br, 1H, $MeC_5\mathit{H}_4$), 4.24 (br, 2H, $MeC_5\mathit{H}_4$), 4.15 (br, 1H, $MeC_5\mathit{H}_4$), 4.03 (s, 1H, SiH), 4.00 (br, 1H, $MeC_5\mathit{H}_4$), 3.87 (br, 1H, $MeC_5\mathit{H}_4$), 3.73 (br, 1H, $MeC_5\mathit{H}_4$), 1.59 (s, 3H, MeC_5H_4), 1.40 (s, 9H, CMe_3), 1.26 (s, 9H, CMe_3), −7.68 (s, 1H, MoH)	98.2 ($Me\mathit{C}_5H_4$), 90.9 ($Me\mathit{C}_5H_4$), 85.1 ($Me\mathit{C}_5H_4$), 83.6 ($Me\mathit{C}_5H_4$), 81.2 ($Me\mathit{C}_5H_4$), 79.4 ($Me\mathit{C}_5H_4$), 79.4 ($Me\mathit{C}_5H_4$), 77.9 ($Me\mathit{C}_5H_4$), 76.4 ($Me\mathit{C}_5H_4$), 73.4 ($Me\mathit{C}_5H_4$), 34.0 ($C(\mathit{Me})$), 33.4 ($C(\mathit{Me})$), 27.1 ($\mathit{C}(Me)_3$), 26.5 ($\mathit{C}(Me)_3$), 15.4 ($\mathit{Me}C_5H_4$), 15.0 ($\mathit{Me}C_5H_4$)
7	$Cp_2Mo(H)(Si(\mathit{t}\text{-}Bu)_2Cl)$	4.36 (s, 5H, Cp), 4.20 (s, 5H, Cp), 1.43 (s, 9H, CMe_3), 1.24 (s, 9H, CMe_3), −7.61 (s, 1H, MoH)	81.7 (Cp), 79.6 (Cp), 32.7 ($\mathit{C}(Me)_3$), 32.2 ($C(\mathit{Me})_3$), 32.1 ($C(\mathit{Me})_3$), 31.6 ($\mathit{C}(Me)_3$)
8	$Cp_2W(H)(SiMe_2Cl)$	4.09 (s, 10H, Cp), 0.30 (s, 6H, $SiMe_2$), −11.48 (s, 1H, WH)	75.9 (Cp), 14.4 ($SiMe_2Cl$)
9	$Cp_2W(H)(SiMe_3)$	4.03 (s, 10H, Cp), 0.46 (s, 9H, $SiMe_3$), −11.13 (s, 1H, WH)	73.8 (Cp), 9.7 ($SiMe_3$)
11	$Cp_2W(SiMe_3)_2$	3.87 (s, 10H, Cp), 0.40 (s, 18H, $SiMe_3$)	77.3 (Cp), 9.5 ($SiMe_3$)
12	$Cp_2W(SiMe_3)(SiMe_2Cl)$	4.01 (s, 10H, Cp), 0.86 (s, 6H, $SiMe_2Cl$), 0.28 (s, 9H, $SiMe_3$)	79.4 (Cp), 12.9 ($SiMe_2Cl$), 9.2 ($SiMe_3$)
13	$Cp_2W(SiMe_3)(Si(\mathit{i}\text{-}Pr)_2Cl)$	4.05 (s, 10H, Cp), 1.43 (m, 2H, $C\mathit{H}(Me)_2$), 1.29 (d, 6H, $CH(\mathit{Me})_2$), 1.21 (d, 6H, $CH(\mathit{Me})_2$), 0.49 (s, 9H, $SiMe_3$)	78.3 (Cp), 25.3 ($\mathit{C}H(Me)_2$), 22.2 ($CH(\mathit{Me})_2$), 21.6 ($CH(\mathit{Me})_2$), 9.5 ($SiMe_3$)
14	$Cp_2W(SiMe_3)(Si(\mathit{t}\text{-}Bu)_2H)$	4.06 (br, 10H, Cp), 3.85 (s, 1H, Si–H), 1.18 (br, 18H, *t*-Bu), 0.42 (s, 9H, $SiMe_3$)	79.5 (Cp),^{b} 75.4 (Cp), 34.6 ($C\mathit{Me}_3$), 33.2 ($C\mathit{Me}_3$) 28.0 ($\mathit{C}Me_3$) 26.6 ($\mathit{C}Me_3$), 9.8 (br $SiMe_3$)
14^c	$Cp_2W(SiMe_3)(Si(\mathit{t}\text{-}Bu)_2H)$	4.01 (s, 5H, Cp), 3.96 (s, 1H, Si–H), 3.80 (s, 5H, Cp), 1.46 (s, 9H, *t*-bu), 1.18 (s, 9H, *t*-Bu), 0.79 (s, 3H, SiMe), 0.68 (s, 3H, SiMe), 0.41 (s, 3H, SiMe)	

^{a} Chemical shifts in ppm relative to $SiMe_4$; coupling constants in hertz. Recorded at 25 °C, unless stated otherwise. ^{b} At −20 °C. ^{c} At −80 °C.

Moorhouse.[12a] Harrod and co-workers have also reported the synthesis of phenylsilyl derivatives by the photolysis of Cp_2MoH_2 in the presence of the corresponding hydridosilanes.[12b]

Formation of group 6 bis(silyl) complexes $Cp_2M(SiR_3)_2$ is a considerably greater synthetic challenge than the silyl hydrides. The most straightforward route, oxidative addition of $Me_3SiSiMe_3$ to photochemically generated Cp_2M is not successful. Furthermore, Schubert and Schenkel reported that attempts to react Cp_2WCl_2 with 2 equiv of $LiSiR_3$ resulted in ring-silylation rather than the desired bis(silyl) complex (eq 1).[13] However, we

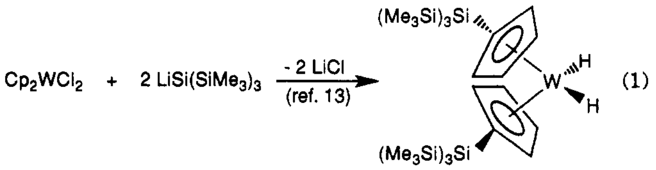

(1)

recently found that the tungstenocene silene complex $Cp_2W(\eta^2\text{-}CH_2{=}SiMe_2)$ reacts cleanly with $HSiMe_3$ to yield the bis(trimethylsilyl) complex,[3] and indeed, this route has proven to be general for a wide range of hydridosilanes.

Results and Discussion

Synthesis of Group 6 Silyl Hydride Complexes, $Cp_2M(H)(SiR_3)$. Photolysis at 350 nm of benzene solutions of the molybdenocene dihydride Cp_2MoH_2 (**1**) in the presence of a variety of hydridosilanes produces H_2 and the corresponding silyl hydride complex in good to excellent yields following sublimation (eq 2). For example,

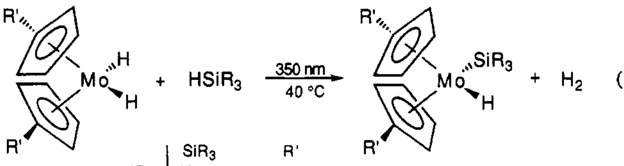

(2)

	SiR_3	R'
3	$SiMe_2H$	H
4a	$SiMe_2Cl$	H
5a	$SiMe_3$	H
5b	$SiMe_3$	CH_3
6a	$Si(\mathit{t}\text{-}Bu)_2H$	H
6b	$Si(\mathit{t}\text{-}Bu)_2H$	CH_3
7	$Si(\mathit{t}\text{-}Bu)_2Cl$	H

treatment of **1** with Me_2SiH_2 in benzene results in no reaction at room temperature in room light over a period of 1 day. However, under photolytic conditions (350 nm) the silyl hydride $Cp_2Mo(H)(SiMe_2H)$ (**3**) is formed within 20 h. A variety of silyl complexes have been prepared using this procedure (eq 2). The methylcyclopentadienyl derivatives **5b** and **6b** were readily prepared from Cp'_2MoH_2 and the appropriate hydridosilane.

Compounds **3**–**7** are all yellow, air- and moisture-sensitive solids which sublime readily at 50–70 °C under high vacuum. The ^{1}H, ^{13}C, and ^{29}Si NMR data of these compounds are listed in Tables 1 and 2, and other analytical data are listed in the Experimental Section. In addition, the solid-state structures of **3**, **4**, **5b**, and **6b** have been determined by single-crystal X-ray diffraction studies (vide infra).

Although there was initially some question whether the electrophilic molybdenum center would be compatible with

---

[12] (a) Cardoso, A. M.; Clark, R. J. H.; Moorhouse, S. *J. Organomet. Chem.* **1980**, *186*, 241. (b) Aitken, C.; Barry, J.-P.; Gauvin, F.; Harrod, J. F.; Malek, A.; Rousseau, D. *Organometallics* **1989**, *8*, 1732.

[13] Schubert, U.; Schenkel, A. *Chem. Ber.* **1988**, *121*, 939.

Table 2. ^{29}Si NMR Data for Molybdenum and Tungsten Silyl Complexes

no.	compound	δ^a	$\delta(HSiR_3)^a$	$\Delta\delta^b$	$^1J_{W-Si}{}^a$
3	$Cp_2Mo(H)(SiMe_2H)$	19.9	−37.7	57.6	
4a	$Cp_2Mo(H)(SiMe_2Cl)$	86.4	11.1	75.3	
4b	$Cp_2Mo(Cl)(SiMe_2Cl)$	70.6	11.1	59.5	
5a	$Cp_2Mo(H)(SiMe_3)$	27.0	−16.3	43.3	
5b	$Cp'_2Mo(H)(SiMe_3)$	27.8	−16.3	44.1	
6a	$Cp_2Mo(H)(Si(t\text{-}Bu)_2H)$	66.8	2.0	64.8	
6b	$Cp'_2Mo(H)(Si(t\text{-}Bu)_2H)$	68.2	2.0	66.2	
7	$Cp_2Mo(H)(Si(t\text{-}Bu)_2Cl)$	108.3	27.6	80.7	
8	$Cp_2W(H)(SiMe_2Cl)$	55.8	11.1	44.7	118
9	$Cp_2W(H)(SiMe_3)$	0.5	−16.3	16.8	84
11	$Cp_2W(SiMe_3)_2$	3.3	−16.3	19.6	106
12	$Cp_2W(SiMe_3)(SiMe_2Cl)$	70.0 ($SiMe_2Cl$)	11.1	58.9	141
		4.5 ($SiMe_3$)	−16.3	20.8	100
13	$Cp_2W(SiMe_3)(Si(i\text{-}Pr)_2Cl)$	70.7 ($Si(i\text{-}Pr)_2Cl$)	24.7	46.0	144
		2.7 ($SiMe_3$)	−16.3	19.0	102
14	$Cp_2W(SiMe_3)(Si(t\text{-}Bu)_2H)$	38.8 ($Si(t\text{-}Bu)_2H$)	2.0	36.8	118
		−3.3 ($SiMe_3$)	−16.3	13.0	111

[a] ^{29}Si Chemical shifts in ppm relative to $SiMe_4$; coupling constants in hertz. [b] $\delta(^{29}Si)$ of silyl complex, $MSiR_3$, relative to the corresponding hydridosilane, $HSiR_3$.

silyl groups containing electronegative substituents such as chloride on silicon, the formation and stability of compounds $Cp_2Mo(H)(SiMe_2Cl)$ (**4a**) and $Cp_2Mo(H)(Si(t\text{-}Bu)_2Cl)$ (**7**) indicates that this is not a problem. The Si–Cl functionality in these complexes is synthetically useful for the further derivatization of the silyl group.[3b,14]

Photolysis of Cp_2MoH_2 in the presence of Me_3SiD yields only the MoD derivative, $Cp_2Mo(D)(SiMe_3)$, and H_2; HD was not detected (eq 3). This result is consistent with a mechanism involving concerted photolytic reductive elimination of H_2 and subsequent thermal oxidative addition of Me_3SiD to the 16e$^-$ molybdenocene fragment. Such a process is in accord with extensive previous studies.[15,16]

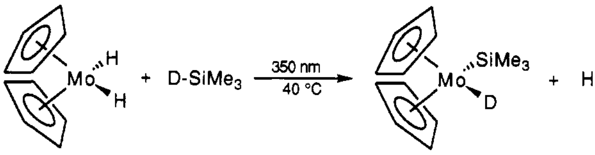

(3)

1 5a-d_1

This general synthetic procedure can also be applied to the preparation of tungsten silyl hydride complexes (eq 4). However, photolytic reactions of Cp_2WH_2 (**2**) require much longer exposure times and generally result in lower yields than the molybdenum analog. The reactions are extremely slow using 350-nm light and only marginally faster using 254 nm. This is in accord with reports by Geoffroy and Bradley that the quantum yield (366 nm) for H_2 extrusion from Cp_2WH_2 is one-tenth that for Cp_2MoH_2.[16] The reaction times can be reduced somewhat by increasing the silane concentration and removing evolved H_2 periodically. Furthermore, Green and co-workers have demonstrated that tungstenocene insertion into arene C–H bonds is quite facile.[11e,i] Therefore, arenes such as benzene and toluene are not suitable solvents for the preparation of tungstenocene silyl hydride complexes, as formation of $Cp_2W(H)(Ar)$ is competitive with the silyl.

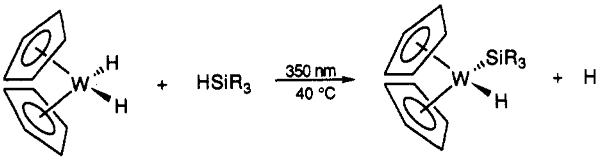

(4)

2 $SiR_3 = SiMe_2Cl$, **8**; $SiMe_3$, **9**

For example, photolysis (350 nm) of Cp_2WH_2 in neat $Me_2Si(H)(Cl)$ for 11 days and with periodic removal of hydrogen results in the formation of $Cp_2W(H)(SiMe_2Cl)$ (**8**) (50% isolated yield). The trimethylsilyl derivative $Cp_2W(H)(SiMe_3)$ (**9**) has also been prepared by photolysis of Cp_2WH_2 and Me_3SiH in cyclohexane solution. Analytical data for these compounds are reported in the Experimental Section, and NMR data are listed in Tables 1 and 2.

Compound **9** has also been be prepared nearly quantitatively by the hydrogenation of the tungstenocene silene complex $Cp_2W(\eta^2\text{-}CH_2{=}SiMe_2)$ (**10**) (eq 5).[3] Although this product is formally the result of net addition of H_2 to a W–C bond in the silene complex, a more complex mechanism appears to be operative (vide infra).

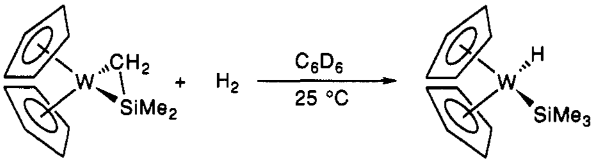

(5)

10 9

As is the case for many metal hydride complexes, clean conversion to the corresponding chlorides can be achieved by treatment with halocarbons such as CCl_4.[2,3,17] For example, treatment of a benzene solution of **4a** with CCl_4 results in the formation of the chloro derivative $Cp_2Mo(Cl)(SiMe_2Cl)$ (**4b**) in 75% isolated yield (eq 6). Although

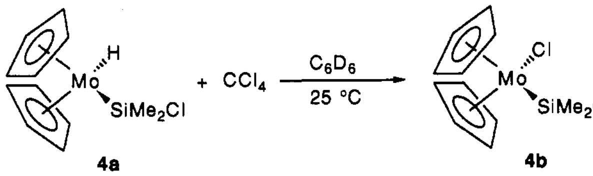

(6)

4a 4b

---

[14] Koloski, T. S.; Pestana, D. C.; Carroll, P. J.; Berry, D. H. Manuscript in preparation.

[15] (a) Perutz, R. N.; Scaiano, J. C. *J. Chem. Soc., Chem. Commun.* **1984**, 457. (b) Cox, P. A.; Grebenik, P.; Perutz, R. N.; Robinson, M. D.; Grinter, R.; Stern, D. R. *Inorg. Chem.* **1983**, *22*, 3614. (c) Chetwynd, T. J.; Grebenik, P.; Perutz, R. N. *Inorg. Chem.* **1982**, *21*, 36477. (d) Grebenik, P.; Downs, A. J.; Green, M. L. H.; Perutz, R. N. *J. Chem. Soc., Chem. Commun.* **1979**, 742.

[16] (a) Geoffroy, G. L.; Bradley, M. G. *Inorg. Chem.* **1978**, *17*, 2410. (b) Geoffroy, G. L.; Bradley, M. G.; Pierantozzi, R. *Adv. Chem. Ser.* **1977**, 181.

[17] Green, M. L. H.; Jones, D. J. *Adv. Inorg. Chem. Radiochem.* **1965**, *7*, 115.

Scheme 1

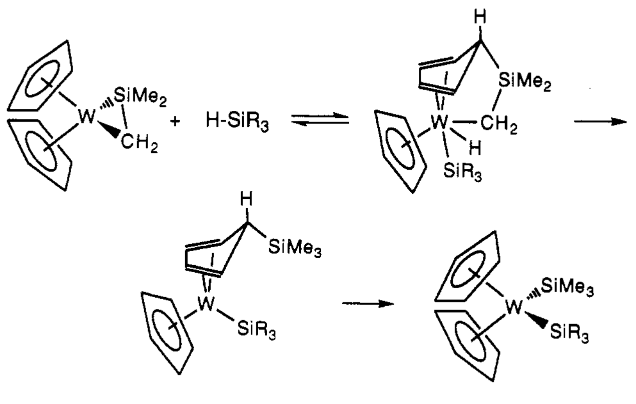

successful for most of the molybdenum and tungsten silyl hydride complexes described above, this reaction is limited somewhat by steric considerations. Thus the bulky silyl hydride complex $Cp_2Mo(H)(Si(t\text{-}Bu)_2Cl)$ (7) is unreactive toward CCl_4, $CHCl_3$, CH_3Cl, CH_3Br, and CH_3I at 25 °C, and decomposes under more forcing conditions.

Synthesis of Bis(silyl) Complexes of Tungsten, $Cp_2W(SiMe_3)(SiR_3)$. It was previously reported that the silene complex **10** reacts with Me_3SiH at 25 °C to cleanly yield the bis(silyl) complex $Cp_2W(SiMe_3)_2$ (**11**) as shown in eq 7. This product is the net result of H–Si addition across the W–C bond of **10**, but a more complicated mechanism has been proposed as shown in Scheme 1.[3] In the proposed mechanism, a coordinatively unsaturated intermediate is generated by reversible migration of the silene silicon to the Cp ring, followed by Si–H oxidative addition and C–H reductive elimination to yield the unsaturated silyl-substituted η^4-cyclopentadiene complex. Migration of the *endo*-$SiMe_3$ group back to the tungsten completes the process.

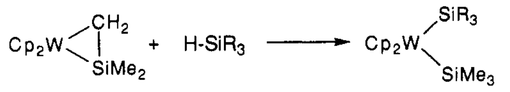

(7)

10

	SiR_3
11	$SiMe_3$
12	$SiMe_2Cl$
13	$Si(i\text{-}pr)_2Cl$
14	$Si(t\text{-}Bu)_2H$

This reaction can also be extended to a variety of silanes to yield unsymmetrical complexes $Cp_2W(SiMe_3)(SiR_3)$ (SiR_3 = $SiMe_2Cl$, **12**; $Si(i\text{-}Pr)_2Cl$, **13**; $Si(t\text{-}Bu)_2H$, **14**). Products **11–13** are formed under relatively mild conditions (ca. 2 equiv of silane, 25 °C). The reactions are complete within 2 days. However, the formation of **14** requires heating to 65 °C in neat silane. Furthermore, the steric requirements in **14** appear to be an upper limit for this system: Reaction of **10** with $(t\text{-}Bu)_2Si(H)Cl$ does not occur up to 75 °C, at which point the silene complex **10** decomposes. This lack of reactivity is most certainly due to the steric hindrance of $(t\text{-}Bu)_2Si(H)Cl$, given that the reaction of **10** with $(i\text{-}Pr)_2Si(H)Cl$ gives **13** in good yields.

The bis(silyl) complexes (**11–14**) have been isolated in high yields as yellow crystalline solids and have been fully characterized. NMR data are listed in Tables 1 and 2. In addition, **13** and **14** have been structurally characterized (vide infra). The major limitation to this reaction as a general route to tungsten bis(silyl) complexes is that the product complex always contains at least one $SiMe_3$ group, as derived from the original silene ligand. Of course, this limitation could potentially be circumvented by preparing complexes of different silene ligands.

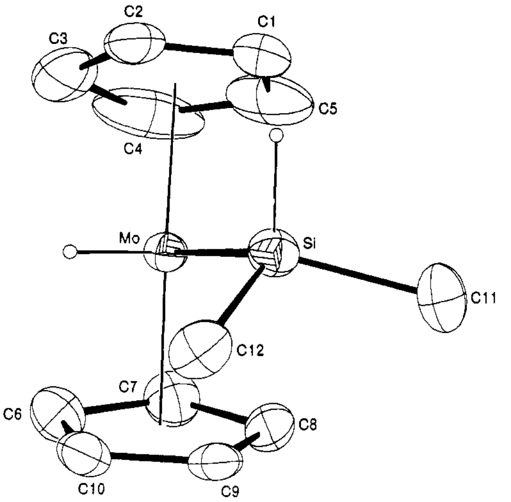

Figure 1. ORTEP drawing of $Cp_2Mo(H)(SiMe_2H)$, **3**, showing 30% probability thermal ellipsoids.

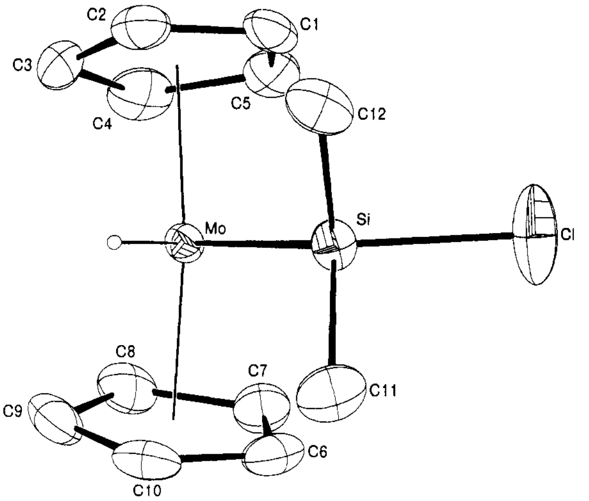

Figure 2. ORTEP drawing of $Cp_2Mo(H)(SiMe_2Cl)$, **4a**, showing 30% probability thermal ellipsoids.

In addition to their value as model compounds, the bis(silyl) complexes have been found to undergo interesting intramolecular redistribution reactions in which alkyl groups migrate between adjacent silicon centers. Studies of these transformations are the subject of a separate report.[14]

Structural Characterization of Silyl and Bis(silyl) Complexes. The mono(silyl) hydride complexes **3**, **4a**, **5b**, **6b**, and **9** have been structurally characterized by single-crystal X-ray diffraction methods. ORTEP drawings showing 30% probability thermal ellipsoids are shown in Figures 1–5, and the structure determinations are summarized in Tables 3 and 4. Selected geometrical parameters are listed in Tables 5 and 6. The structures of these compounds are very similar, and exhibit the pseudotetrahedral geometry typical of bent metallocenes, with the metal, silicon, and metal hydrides lying in a plane perpendicular to the plane containing the metal and the two Cp ring centroids. Compound **3** crystallizes with two unique, but statistically equivalent, molecules in the unit cell. Only one of the unique molecules of **3** is depicted in Figure 1. Trimethylsilyl complexes **5b** and **9**, are isomorphous (space group *Pnma*) and both exhibit crystallographically imposed mirror symmetry. The Mo, Si, C8, and hydride atoms in **5b** and the W, Si, C6 and hydride atoms in **9** are coplanar and lie on the mirror plane between the two Cp ligands. The positions of the silicon and

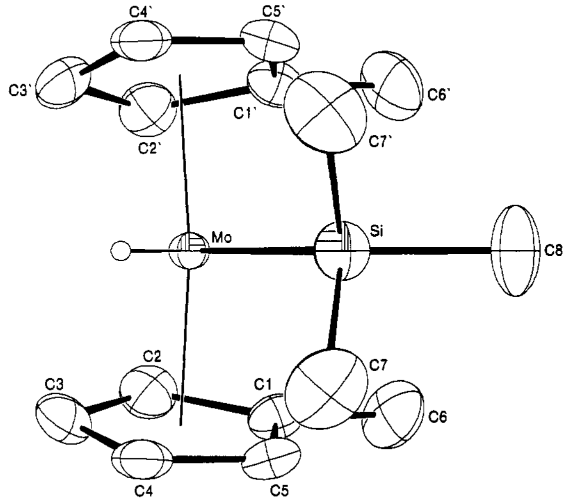

Figure 3. ORTEP drawing of $Cp'_2Mo(H)(SiMe_3)$, **5b**, showing 30% probability thermal ellipsoids.

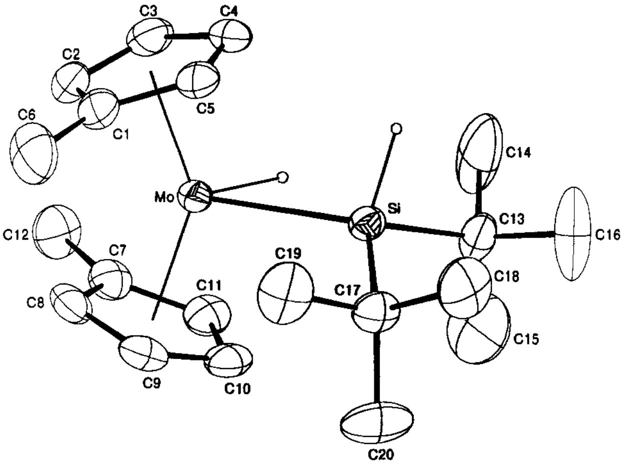

Figure 4. ORTEP drawing of $Cp'_2Mo(H)(Si(t\text{-}Bu)_2H)$, **6b**, showing 30% probability thermal ellipsoids.

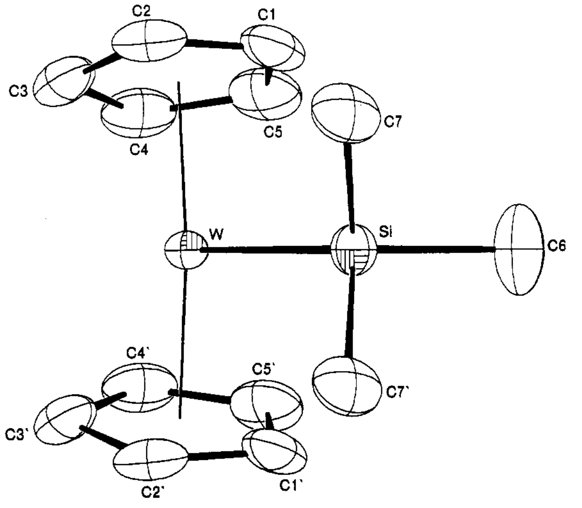

Figure 5. ORTEP drawing of $Cp_2W(H)(SiMe_3)$, **9**, showing 30% probability thermal ellipsoids.

molybdenum hydrides in **3**, **4a**, **5b**, and **6b** were located from electron density maps and were succesfully refined. Although the hydrides refined to chemically reasonable locations, the usual cautions regarding the accuracy of hydrogen positions determined by X-ray diffraction studies apply. The tungsten hydride in **9** was not located.

The M–Si bond lengths for these molybdenum and tungsten silyl hydride complexes fall in the range 2.513(1) to 2.604(1) Å, which is reasonable for Mo– and W–Si single bonds based on covalent radii of the two atoms,[18,19] but is somewhat shorter than the range of 2.614–2.652 Å observed in four non-metallocene molybdenum and tungsten complexes with nonbridging silyls.[20] There is an excellent agreement between the M–Si bond distances in the molybdenum $SiMe_3$ derivative **5b** and tungsten analog **9** (2.560(1) Å in both structures), despite the methyl groups on the Cp rings of the former. There is also good correlation between the size of the silyl ligand and the M–Si bond distance. Thus **6b**, which contains the most sterically demanding silyl, $Si(t\text{-}Bu)_2H$, exhibits the longest M–Si bond distance (2.604(1) Å), whereas the M–$SiMe_2H$ distance in **3** is significantly shorter (2.539(2) Å average), and the M–$SiMe_3$ distances in **5b** and **9** are intermediate.

The M–Si distance in the silyl hydride complexes is not determined by steric factors alone. The shortest Mo–Si bond distance is observed in the $SiMe_2Cl$ derivative, **4a** (2.513(1) Å), even though the silicon is more hindered than in **3**. In addition, the Si–Cl bond length in **4a** (2.158(1) Å) is considerably longer than in typical organic chlorosilanes (2.023 Å).[21] The relatively short M–Si and long Si–Cl bond distances are the result of two effects. Firstly, the electronegative chloride will tend to form bonds using a high degree of silicon p-orbital character (Bent's rule).[22] This leaves a correspondingly high percentage of silicon s-orbital character for bonding with the electropositive metal, which results in a stronger M–Si bond.

The chlorosilyl also exhibits a particularly strong M–Si interaction as a result of π-back bonding from the d^2 metal center to the silicon. Although it is generally accepted that the d-orbitals on main group elements such as silicon are too diffuse and high in energy to play a primary role as electron acceptors, the Si–Cl σ^* orbital in **4a** is also of the appropriate symmetry for π-backbonding.[23] Significantly, the Si–Cl bond in the solid-state structure of **4a** lies in the equatorial plane between the Cp ligands (H–Mo–Si–Cl torsional angle = 174.5°) and is thus aligned for maximum overlap with the HOMO on the metal.[24] Metal–

---

[18] The covalent radius of silicon is 1.17–1.18 Å.[19a] The radii of tungsten and molybdenum have been variously estimated as 1.30–1.60 Å.[19] It is assumed in the discussion that the radii of Mo and W are virtually identical.

[19] (a) Pauling, L. *The Nature of the Chemical Bond*, 3rd ed.; Cornell University Press: Ithaca, NY, 1960. (b) Pauling, L. *Proc. Nat. Acad. Sci. U.S.A.* **1975**, *72*, 3799–3801. (c) Chisholm, M. H.; Corning, J. F.; Huffman, J. C. *Inorg. Chem.* **1983**, *22*, 38. (d) Churchill, M. R.; Fennessey, J. P. *Inorg. Chem.* **1968**, *5*, 953–959.

[20] (a) Sharma, S.; Kapoor, R. N.; Cervantes-Lee, F.; Pannell, K. H. *Polyhedron* **1991**, *10*, 1177. (b) Darensbourg, D. J.; Bauch, C. G. B.; Reibenspies, J. H.; Rheingold, A. L. *Inorg. Chem.* **1988**, *27*, 4203. (c) Heyn, R. H.; Tilley, T. D. *Inorg. Chem.* **1990**, *29*, 4051. (d) Chisholm, M. H.; Chiu, H. T.; Folting, K.; Huffman, J. C. *Inorg. Chem.* **1984**, *23*, 4097. (e) This analysis does not include the W–Si distance in $W(H)_2(I)(PMe_3)_3(SiMe_3)$, which was reported as 2.388(6) Å. This unreasonable value is much shorter than the observed W–PMe_3 distances, and is almost certainly incorrect: Barron, A. R.; Wilkinson, G.; Motevalli, M.; Hursthouse, M. B. *J. Chem. Soc., Dalton Trans.* **1987**, 837.

[21] Lukevics, E.; Pudova, O.; Sturkovich, R. In *Molecular Structure of Organosilicon Compounds*; Ellis Horwood Ltd., New York, 1989.

[22] Bent, H. A. *Chem. Rev.* **1961**, *61*, 275.

[23] Although the question of d-orbital participation in main group element bonding was once controversial, there is now little disagreement among theoretical chemists that it does not play a major role. Reference a offers a particularly cogent summary. (a) Massey, A. G. *Main Group Chemistry*; Ellis Horwood: New York, 1990; Chapter 1. (b) Orpen, A. G.; Connelly, N. G. *J. Chem. Soc., Chem. Commun.* **1985**, 310. (c) Kutzelnigg, W. *Angew. Chem., Int. Ed. Engl.* **1984**, *23*, 272. (d) Reed, A. E.; Weinhold, F. *J. Am. Chem. Soc.* **1986**, *108*, 3586. (e) Luke, B. T.; Pople, J. A.; Krogh-Jespersen, M. B.; Apeloig, Y.; Chandrasekhar, J.; Schleyer, P. v. R. *J. Am. Chem. Soc.* **1986**, *108*, 260.

[24] (a) Lauher, J. W.; Hoffmann, R. *J. Am. Chem. Soc.* **1976**, *98*, 1729. (b) Peterson, J. L.; Lichtenberger, D. L.; Fenske, R. F.; Dahl, L. F. *J. Am. Chem. Soc.* **1975**, *97*, 6433. (c) Brintzinger, H. H.; Lohr, L. L., Jr.; Tang Wong, K. L. *J. Am. Chem. Soc.* **1975**, *97*, 5146. (d) Green, J. C.; Green, M. L. H.; Prout, C. K. *J. Chem. Soc., Chem. Commun.* **1972**, 421.

Table 3. Summary of Structure Determinations[a] of Molybdenum Silyl Complexes 3, 4a, 5b, and 6b

compound	3	4a	5b	6b
formula	$MoC_{12}H_{18}Si$	$MoClSiC_{12}H_{17}$	$MoSiC_{15}H_{24}$	$MoSiC_{20}H_{34}$
formula weight	286.30	320.75	328.38	398.52
crystal dimensions (mm)	0.03 × 0.23 × 0.63	0.18 × 0.30 × 0.40	0.40 × 0.35 × 0.38	0.24 × 0.32 × 0.36
crystal glass	orthorhombic	monoclinic	orthorhombic	monoclinic
space group	*Pbca* (No. 61)	$P2_1/n$ (No. 14)	*Pnma* (No. 62)	$P2_1/n$ (No. 14)
Z	16	4	4	4
cell constants				
a (Å)	7.755(1)	11.876(4)	13.613(1)	14.926(3)
b (Å)	22.026(2)	8.575(1)	13.031(1)	9.117(1)
c (Å)	29.191(5)	13.785(3)	8.658(1)	105.34(1)
β (deg)		112.08(3)		105.34(1)
V (Å^3)	4986(2)	1301(1)	1535.9(4)	2045(1)
μ (cm^{-1})	10.85	12.50	8.90	6.80
transmission (%)(min, max, avg)[b]	–	–	97.84, 99.98, 99.15	–
D_{calcd} (g cm^{-3})	1.526	1.638	1.42	1.294
F(000)	2336	648	680	840
h,k,l collected	10, 28, 37	±15, 11, 17	17, 11, 16	19, –11, ±20
no. of reflections measured	6398	3297	2038	5173
no. of unique reflections	5699	3170	1836	4687
no. of reflections used in refinement ($F^2 > 3.0\sigma$)	2785	2966	1560	3626
no. of parameters	253	187	82	199
data/parameter ratio	11.0	15.9	19.0	18.2
R_1	0.042	0.037	0.025	0.032
R_2	0.049	0.040	0.035	0.045
GOF	1.377	4.528	1.255	1.470

[a] Radiation: Mo Kα (λ = 0.71073 Å); range = 2.0–27.5°; scan mode ω–2θ. [b] Absorption correction (ψ scans) when applied.

Table 4. Summary of Structure Determinations[a] of Tungsten Silyl Complexes 9 and Tungsten Bis(silyl) Complexes 13 and 14

compound	9	13	14
formula	$WSiC_{13}H_{20}$	$WC_{19}H_{33}Si_2Cl$	$WSi_2C_{21}H_{38}$
formula weight	388.24	536.95	530.56
crystal dimensions (mm)	0.55 × 0.30 × 0.20	0.10 × 0.23 × 0.70	0.40 × 0.28 × 0.25
crystal class	orthorhombic	monoclinic	monoclinic
space group	*Pnma* (No. 62)	$P2_1/n$ (No. 14)	*C*2/*c* (No. 15)
Z	4	4	8
cell constants			
a (Å)	11.954(1)	9.502(1)	36.014(1)
b (Å)	12.766(1)	14.829(2)	8.908(2)
c (Å)	8.744(2)	15.069(2)	14.131(4)
β (deg)		96.74(1)	98.08(1)
V (Å^3)	1334.5(5)	2108.5(8)	4488(1)
μ (cm^{-1})	89.01	58.35	53.64
transmission (%)(min, max, avg)[b]	50.20, 99.97, 81.78	34.24, 99.91, 74.00	–
D_{calcd} (g cm^{-3})	1.932	1.691	1.570
F(000)	744	1064	2128
h, k, l collected	15, ±11, 16	12, –19, ±19	±11, –18, ±24
no. of reflections measured	3344	5325	10695
no. of unique reflections	1595	4833	5157
no. of reflections used in refinement ($F^2 > 3.0\sigma$)	1381	3974	3991
no. of parameters	73	208	217
data/parameter ratio	18.9	19.1	18.4
R_1	0.020	0.026	0.023
R_2	0.026	0.036	0.029
GOF	0.950	1.367	0.966

[a] Radiation: Mo Kα (λ = 0.71073 Å); θ range = 2.0–27.5°; scan mode ω–2θ. [b] Absorption correction (ψ scans) when applied.

silicon backbonding would increase the effective M–Si bond order, and by populating the Si–Cl σ^* orbital, decrease the Si–Cl bond order. In valence bond terms, this type of interaction ("hyperconjugation") is represented by the contribution of the "no-bond" resonance structure as shown in Scheme 2. In the limiting case, the complex would be a cationic silylene complex with a fully dissociated chloride counterion and would be sp^2 hybridized at silicon.[25] In a more intermediate situation it could be viewed as a base-stabilized silylene,[9a,26] where the chloride anion is acting as the Lewis base. Further evidence supporting some degree of silylene character is found in the ^{29}Si data (vide infra). Although the ground-state structure of **4a** is principally that of a metal–silicon single bond, silylene character does appear to be important in determining the reaction chemistry of the chlorosilyl complexes.[14]

The solid state structures of the bis(silyl) complexes **13** and **14** were also determined by single crystal X-ray

---

(25) (a) Straus, D. A.; Grumbine, S. D.; Tilley, T. D. *J. Am. Chem. Soc.* **1990**, *112*, 7801. (b) Grumbine, S. D.; Tilley, T. D.; Rheingold, A. L. *J. Am. Chem. Soc.* **1993**, *115*, 358. (c) Grumbine, S. D.; Tilley, T. D.; Rheingold, A. L.; Arnold, F. P. *J. Am. Chem. Soc.* **1993**, *115*, 7884.

(26) (a) Straus, D. A.; Tilley, T. D.; Rheingold, A. L.; Geib, S. J. *J. Am. Chem. Soc.* **1987**, *109*, 5872. (b) Straus, D. A.; Zhang, C.; Quimbita, G. E.; Grumbine, S. D.; Heyn, R. H.; Tilley, T. D.; Rheingold, A. L.; Geib, S. J. *J. Am. Chem. Soc.* **1990**, *112*, 2673. (c) Grumbine, S. D.; Chadha, R. K.; Tilley, T. D. *J. Am. Chem. Soc.* **1992**, *114*, 1518. (d) Zybill, C.; Müller, G. *Angew. Chem. Int. Ed. Engl.* **1987**, *26*, 669. (e) Zybill, C.; Wilkinson, D.; Müller, G. *Angew. Chem. Int. Ed. Engl.* **1988**, *27*, 583. (f) Zybill, C.; Müller, G. *Organometallics* **1988**, *7*, 1368. (g) Zybill, C.; Wilkinson, D.; Leis, C.; Müller, G. *Angew. Chem. Int. Ed. Engl.* **1989**, *28*, 203. (h) Leis, C.; Zybill, C.; Lachmann, J.; Müller, G. *Polyhedron* **1991**, *11*, 1163. (i) Zybill, C. *Top. Curr. Chem.* **1991**, *160*, 1. (j) Probst, R.; Leis, C.; Gamper, E.; Herdtweck, E.; Zybill, C. *Angew. Chem. Int. Ed. Engl.* **1991**, *30*, 1132. (k) Leis, C.; Wilkinson, D.; Handwerker, H.; Zybill, C.; Müller, G. *Organometallics* **1992**, *11*, 514.

Table 5. Selected Bond Lengths (Å) in Mono(silyl) Complexes of Molybdenum and Tungsten

compound	M–Si		M–HM	Si–C		Si–X	
3[a]	Mo–Si	2.538(2)	1.72(6)	Si–C11	1.866(9)	Si–HSi	1.33(7)
				Si–C12	1.873(8)		
	Mo–Si′	2.541(2)	1.63(6)	Si′–C11′	1.873(8)	Si′–H′Si′	1.41(9)
				Si′-C12′	1.848(10)		
4a	Mo–Si	2.513(1)	1.83(5)	Si–C11	1.891(4)	Si–Cl	2.158(1)
				Si–C12	1.894(5)		
5b	Mo–Si	2.560(1)	1.71(4)	Si–C7	1.902(4)		
				Si–C8	1.882(6)		
6b	Mo–Si	2.604(1)	1.68(3)	Si–C13	1.952(3)	Si–HSi	1.42(3)
				Si–C17	1.949(3)		
9[b]	W–Si	2.560(1)		Si–C6	1.894(8)		
				Si–C7	1.896(5)		

[a] Two independent molecules in the unit cell. [b] HW not located.

Table 6. Selected Bond Angles (deg) in Mono(silyl) Complexes of Molybdenum and Tungsten

compound	Cp1–M–Cp2[a]	Si–M–HM	M–Si–C		M–Si–X		C–Si–E[b]	
3[c]	147.0	63.4(19)	Mo–Si–C11	116.1(3)	Mo–Si–HSi	108(3)	C11–Si–C12	105.2(4)
			Mo–Si–C12	117.3(3)			C11–Si–HSi	103(3)
	146.6	61.2(20)	Mo′–Si′–C11′	117.0(3)	Mo′–Si′–H′Si′	115(4)	C12–Si–HSi	106(3)
			Mo′–Si′–C12′	117.6(3)			C11′–Si′–C12′	104.6(4)
							C11′–Si′–H′Si′	101(4)
							C12′–Si′-H′Si′	99(4)
4a	145.5	62.2(17)	Mo–Si–C11	118.1(1)	Mo–Si–Cl	113.1(1)	C11–Si–Cl	101.8(2)
			Mo–Si–C12	117.8(1)			C12–Si–Cl	101.8(1)
							C11–Si–Cl2	101.8(2)
5b	146.3	64.9(12)	Mo–Si–C7	115.3(1)			C7–Si–C7′	100.5(2)
			Mo–Si–C8	113.8(3)			C7–Si–C8	105.2(2)
6b	144.4	71.8(12)	Mo–Si–C13	117.3(1)	Mo–Si–HSi	107.2(13)	C13–Si–C17	112.1(1)
			Mo–Si–C17	117.8(1)			C13–Si–HSi	98.4(11)
							C17–Si–HSi	100.2(13)
9[d]	143.0		W–Si–C6	113.6(2)			C6–Si–C7	105.4(2)
			W–Si–C7	115.7(1)			C7–Si–C7′	99.5(2)

[a] Cp1 and Cp2 are the centroids of the η^5-C_5H_5. [b] E ≡ H, Cl, or C atom. [c] There are two independent molecules in the unit cell. [d] HW not located.

Scheme 2

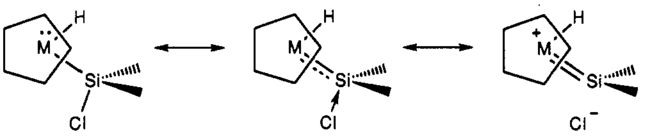

diffraction studies. Crystallographic details are summarized in Table 4. Selected bond distances and angles are listed in Tables 7 and 8. ORTEP drawings, showing 30% probability thermal ellipsoids, are presented in Figures 6 and 7. Compounds **13** and **14** also exhibit a pseudotetrahedral geometry at the tungsten center and are structurally similar to the silyl hydride derivatives. The bulk of the second silyl group is accommodated by longer W–Si bond distances and smaller Cp–W–Cp angles than in the silyl hydrides. For example, the W–$SiMe_3$ distances are ca. 2.60 Å in the bis(silyls) versus 2.560(1) Å in **5b** and **9**. The metal–$Si(t\text{-Bu})_2H$ distance also increases ca. 0.04 Å in going from the silyl hydride **6b** to the bis(silyl) **14**. Furthermore, the Si–W–Si angles in the bis(silyl) complexes are 10–20° larger than corresponding the H–M–Si angles in the silyl hydrides, which also reflects the greater steric congestion in the former. However, as also found for the silyl hydrides, chlorosilyl ligands exhibit relatively short M–Si distances. Thus the W–$Si(i\text{-Pr})_2Cl$) distance in **13** (2.594(1) Å) is actually somewhat shorter than the much less-hindered W–$SiMe_3$ linkage in the same molecule (2.602(1) Å). The steric bulk of the *i*-Pr forces an orientation of the silyl such that the Si–Cl bond does not lie in the equatorial plane (Si–Wi–Si–Cl torsional angle = 70.3°). The inductive effects of the electronegative chloride will lead to shortened M–Si bond distances, regardless of silyl group orientation. However, the degree of W–Si π-bonding involving overlap with the Si–Cl σ^* orbital should be less in **13** than in **4a** (D(M–Si) = 2.513(1) Å), in which the Si–Cl bond is more suitably aligned for back-bonding.

Trends in the ^{29}Si NMR of Molybdenum and Tungsten Silyl Complexes. The resonances of silyl groups in the ^{29}Si NMR spectra of the silyl and bis(silyl) complexes vary over a 110 ppm range (Table 2), but several trends are apparent. First of all, substitution of Cp′ for Cp as in **5a,b** and **6a,b** does not have a major effect on $\delta(^{29}Si)$, and the shifts vary by <2 ppm. On the other hand, changing the metal from molybdenum to tungsten leads to an appreciable shift of the silyl resonance to higher field. For example, the shift for the tungsten derivative is 30.6 ppm upfield of the molybdenum analog in the case of the $SiMe_2Cl$ complexes **4a** and **8**, and 26.5 ppm upfield for the $SiMe_3$ complexes **5a** and **9**. A similar upfield shift of 19.8 ppm has also been noted in the case of the molybdenum and tungsten disilene complexes $Cp_2M(\eta^2\text{-}Me_2Si{=}SiMe_2)$, even though the absolute shifts are quite different than in the simple silyls ($\delta(^{29}Si)$ = −20.3 and −40.1).[2a,b] Note that in each case these pairs of congeners should be essentially isostructural (vide supra), and thus the change in chemical shifts is directly attributable to the metal and not indirect factors such as conformation of the ancillary ligands. In any event, it is clear that tungsten silicon compounds appear to exhibit ^{29}Si resonances ca. 20–30 ppm upfield of the molybdenum derivatives.

In general $\delta(^{29}Si)$ in the complexes also mirrors the shifts observed in the parent silanes, with electron-withdrawing groups on silicon leading to more downfield shifts.[27]

---

[27] Scholl, R. L.; Maciel, G. E.; Musker, W. K. *J. Am. Chem. Soc.* **1972**, *94*, 6376.

Table 7. Selected Bond Lengths (Å) in Bis(silyl) Complexes of Tungsten

compound	W–SiMe$_3$		W–SiR$_2$X		Si–Me$_3$		Si–R$_2$X		Si–X	
13	W–Si1	2.602(1)	W–Si2	2.594(1)	Si1–C11	1.902(5)	Si2–C14	1.930(4)	Si2–Cl	2.149(2)
					Si1–C12	1.913(5)	Si2–C17	1.923(4)		
					Si1–C13	1.905(5)				
14	W–Si2	2.599(1)	W–Si1	2.644(1)	Si2–C19	1.895(6)	Si1–C11	1.979(4)	Si1–HSi	1.42(5)
					Si2–C20	1.892(6)	Si1–C15	1.944(4)		
					Si2–C21	1.914(6)				

Table 8. Selected Bond Angles (deg) in Bis(silyl) Complexes of Tungsten

compound	Cp1–W–Cp1[a]	Si1–W–Si2	W–Si–C		W–Si–X		C–Si–C		C–Si–X	
13	138.8	86.0(1)	W–Si1–C11	117.8(2)	W–Si2–Cl	112.9(1)	C11–Si1–C12	100.4(2)	C14–Si2–Cl	102.0(1)
			W–Si1–C12	113.3(2)			C11–Si1–C13	100.4(2)	C17–Si2–Cl	99.7(1)
			W–Si1–C13	120.1(2)			C12–Si1–C13	101.7(2)		
			W–Si2–C14	117.0(1)			C14–Si2–C17	105.5(2)		
			W–Si2–C17	117.4(1)						
14[b]	140.9	97.3(1)	W–Si1–C11	115.6(1)	W–Si1–HSi	107.5(20)	C11–Si1–C15	108.4(2)	C11–Si1–HSi	99.5(21)
			W–Si1–C15	123.2(1)			C19–Si2–C20	103.1(2)	C15–Si1–HSi	98.3(21)
			W–Si2–C19	120.4(2)			C19–Si2–C21	98.6(3)		
			W–Si2–C20	119.0(2)			C20–Si2–C21	100.6(3)		
			W–Si2–C21	111.6(2)						

[a] Cp1 and Cp2 are the centroids of the η^5-C_5H_5. [b] HSi was located but coordinates were not refined.

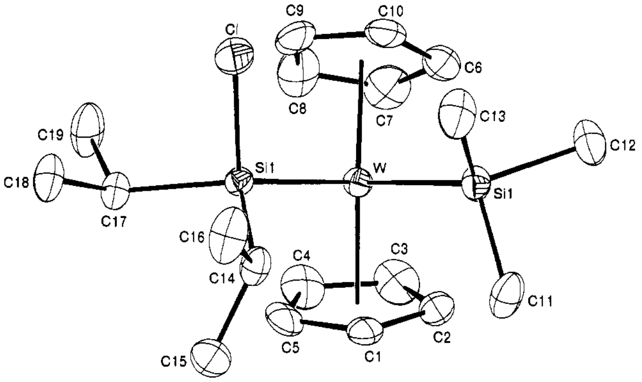

Figure 6. ORTEP drawing of $Cp_2W(SiMe_3)(Si(i\text{-}Pr)_2Cl)$, **13**, showing 30% probability thermal ellipsoids.

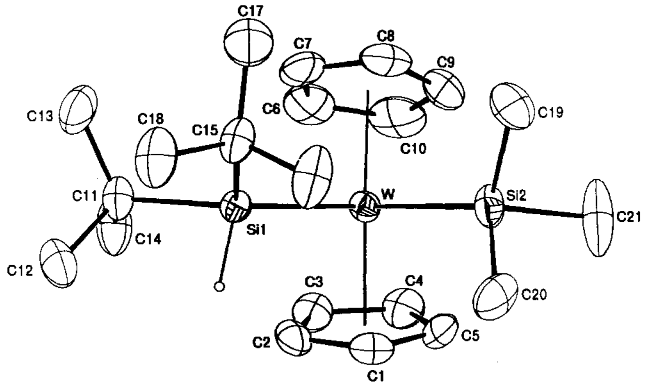

Figure 7. ORTEP drawing of $Cp_2W(SiMe_3)(Si(t\text{-}Bu)_2H)$, **14**, showing 30% probability thermal ellipsoids.

Consider for example, the series $Cp_2Mo(H)(SiMe_2X)$ were X = H, Me, and Cl (**3**, **5a**, and **4a**), which exhibit resonances at 19.9, 27.0, and 86.4 ppm, respectively. Clearly the chloride substitution leads to the biggest perturbation in this series ($\Delta\delta$ ca. 60 ppm), and this is also observed in comparing **8** and **9** ($\Delta\delta$(Me/Cl) = 55.3 ppm), and **11** and **12** ($\Delta\delta$(Me/Cl) = 66.7 ppm). Although this trend is observed in the parent silanes, $HSiR_2X$ (Table 2),[28] the effect of chloride appears to be magnified in the silyl complexes, $MSiR_2X$. For example, $\Delta\delta$(Me/Cl) for $HSiMe_2X$ is only 27.4, or half that in the metal silyls. The large jump in chemical shift may well be due to the partial silylene character possible in the chlorosilyl complexes, as described above.

As a final point regarding $\delta(^{29}Si)$, it is worth noting that the silyl chemical shifts in the tungsten complexes are not particularly sensitive to the nature of the other ligand in the metallocene equatorial wedge. Thus the $SiMe_3$ silicon in the silyl hydride **9** is observed at δ 0.5, whereas the $SiMe_3$ resonances for the bis(silyl) complexes fall in a narrow range from δ −3.3 to +4.5.

Tungsten has one magnetically active isotope, ^{183}W, which has $I = {}^1/_2$ and occurs with 14.4% natural abundance. Satellites due to $^1J_{W-Si}$ can usually be observed in the ^{29}Si spectra of the tungsten silyls, and these values are listed in Table 2. There appear to be two main trends in these tungsten–silicon coupling constants. First, the couplings are uniformly greater in the bis(silyls) **11**–**14** than in the silyl hydrides **8**–**9**. The $^1J_{W-Si}$ in the $SiMe_2Cl$ of **12** is 33 Hz greater than in **8**. Likewise, the coupling constants in the $SiMe_3$ ligands of **11** and **12** are comparable to one another, but are ca. 30 Hz greater than in the corresponding silyl hydride **9**. The second apparent trend in the coupling constants is that a chloride on silicon leads to a increase of >30 Hz in J_{W-Si}. Thus the coupling in **9** is 84 Hz, but $SiMe_2Cl$ derivative **8** exhibits a coupling of 118 Hz. Similarly, the $SiMe_2Cl$ ligand in **12** exhibits a coupling of 141 Hz, 41 Hz greater than the $SiMe_3$ ligand in the same complex.

By far the most significant contribution to the magnitude of one-bond coupling constants is the degree of s-orbital character in the bond; greater % s character correlates with larger coupling constants. Thus, the larger values of J_{W-Si} which are observed in the bis(silyl) complexes imply higher % s orbital character in the W–Si bonds relative to the silyl hydride complexes. Interestingly, there is no obvious correlation between W–$SiMe_3$ bond lengths in the structurally characterized complexes and J_{W-Si}, and, in fact, the largest coupling constant for a $SiMe_3$ ligand is found in **14**, which exhibits the longest W–$SiMe_3$ distance. The most consistent relationship appears to be between the silyl–tungsten–ligand angles and J_{W-Si}. For example, the Si–W–Si angles in **13** and **14** (86.0 and 97.3°) are

---

[28] $\delta(^{29}Si)$ for parent silanes: (a) Loewer, R.; Vongehr, M.; Marsmann, H. C. *Chem. Ztg.* **1975**, *99*, 33. (b) Murphy, P. D.; Taki, T.; Sogabe, T.; Metzler, R.; Squires, T. G.; Gerstein, B. C. *J. Am. Chem. Soc.* **1979**, *101*, 4055. (c) Harris, R. K.; Kimber, B. J. *Magn. Reson.* **1975**, *17*, 174. (d) As measured for this work: $(t\text{-}Bu)_2SiH_2$ δ 2.01; $(t\text{-}Bu)_2SiHCl$ δ 27.61.

considerably larger than the Si–M–H angles in the silyl hydride complexes (ca. 61–72°), and are accompanied by relatively large W–$SiMe_3$ coupling constants of 102 and 111 Hz, respectively. The theoretical basis for this trend lies in the nature of the three valence orbitals in bent metallocenes.[24] Although two of the orbitals are of a_1 symmetry, Lauer and Hoffman calculated that the higher energy orbital ($2a_1$), which is the HOMO for a d^2 configuration, has the highest percentage of s-character.[24a] Furthermore, it has been shown that the relative stabilities of the $1a_1$ and $2a_1$ orbitals, and hence the percentage of each used in forming σ-bonds, vary with the X–M–Y angle. In particular, the $1a_1$ orbital has two angular nodes which can render this orbital nearly nonbonding toward σ-donors at certain X–M–Y angles, but overlap with the nodeless $2a_1$ orbital is relatively independent of the angle. Thus the % s character (% $2a_1$ orbital) in the M–X σ-bonds can also vary substantially with the X–M–Y angle, reaching a maximum at the critical angle at which the $1a_1$ orbital is nonbonding. Although the exact value of the critical angle cannot be determined without a substantially more sophisticated calculation, the qualitative argument regarding the hybridization at the Cp_2W center is sufficient to explain the observed trend in W–Si coupling constants.

The other major influence on the magnitude of J_{W-Si} is the presence of a chloride on silicon. Both the inductive and π-back-bonding effects of chloride substitution as discussed above are expected to lead to greater silicon s-orbital character in the W–Si bond and hence larger coupling constants. Similar trends in tungsten–carbon coupling constants have been observed in tungsten alkyl and carbene complexes.[29]

Solution Dynamic Behavior of Bulky Silyl Complexes 6a, 6b, and 14. In general, the ^1H NMR spectra for the (mono)silyl hydride and bis(silyl) complexes are straightforward. However, complexes containing the bulky $Si(t\text{-}Bu)_2H$ ligands exhibit the room temperature ^1H NMR spectra which are consistent with hindered rotation about the M–Si bond. Therefore, the dynamic behavior of these complexes in solution was investigated by variable-temperature ^1H NMR studies.

The room temperature ^1H NMR spectrum of $Cp_2Mo(H)(Si(t\text{-}Bu)_2H)$, **6a**, in toluene-$d_8$ consists of six resonances: two sharp singlets each for the Cp and *t*-Bu groups and one singlet each for the SiH and MoH groups. The Cp and *t*-Bu groups are rendered inequivalent by the conformation of the silyl group and the hindered rotation about the Mo–$Si(t\text{-}Bu)_2H$ bond. The silyl conformation is most likely the same as that observed in the crystal structure of the MeCp analog, **6b** (Figure 4). Coalescence of the Cp and *t*-Bu resonances was observed at 130 ± 10 °C, although the fast-exchange limit, in which sharp singlets should be observed, was not reached due to decomposition of **6a** at higher temperatures. This value of T_c, in conjunction with $\Delta\nu$ for the resonances in the slow-exchange limit, allows calculation of $\Delta G^{\ddagger}_{rot}$, the barrier to rotation about the Mo–Si bond, as 20.7 ± 0.5 kcal mol^{-1} (Table 9). The MeCp analog **6b** also exhibits inequivalent rings and *t*-Bu groups. Coalescence of the latter was also observed at 130 °C and a value of $\Delta G^{\ddagger}_{rot}$ = 20.6 ± 0.5 kcal mol^{-1} calculated.

Because there was significant decomposition observed during the determination of T_c for compounds **6a** and **6b**, these values should be used with some caution. Another mechanism, such as elimination and readdition of silane, which would also result in equivalent Cp and *t*-Bu resonances, could be operative at these relatively high temperatures. At the very least, however, the values calculated represent a *lower limit* for $\Delta G^{\ddagger}_{rot}$ in **6a** and **6b**, and any uncertainty does not affect the discussion which follows below.

Table 9. Variable-Temperature ^1H NMR Data for M–$Si(t\text{-}Bu)_2H$ Complexes

compound[a]	T_c (°C)	$\Delta G^{\ddagger}_{rot}$[b]	D(M–Si)[c] (Å)
$Cp_2Mo(H)(Si(t\text{-}Bu)_2$, **6a**	130	20.70	
$Cp'_2Mo(H)(Si(t\text{-}Bu)_2H)$, **6b**	130	20.56	2.6044(9)
$Cp_2W(SiMe_3)(Si(t\text{-}Bu)_2H)$, **14**	15	13.50	2.644(1)
$Cp_2Ta(CO)(Si(t\text{-}Bu)_2H)$	40	15.4	2.684(1)
$Cp_2Ta(PMe_3)(Si(t\text{-}Bu)_2H)$	–47	10.9	2.742(2)

[a] Data for the tantalum complexes is taken from ref 30. [b] $\Delta G^{\ddagger}$ for rotation around M–$Si(t\text{-}Bu)_2H$ bond in kcal mol^{-1}. [c] M–$Si(t\text{-}Bu)_2H$ bond length.

The room temperature ^1H NMR spectrum for $Cp_2W(SiMe_3)(Si(t\text{-}Bu)_2H)$, **14**, shows broad resonances centered at δ 4.04 and 1.19 attributable to the Cp and *t*-Bu ligands, a sharp singlet at δ 0.43 for the $SiMe_3$ group, and another singlet at δ 3.85 for the SiH. A stack plot of the ^1H NMR spectra taken at various temperatures in toluene-d_8 is shown in Figure 8. In contrast to **6a,b**, however, coalescence of the $Si(t\text{-}Bu)_2H$ and Cp ligands is observed *below* room temperature, at 15 °C ($\Delta G^{\ddagger}_{rot}$ = 13.5 ± 0.1 kcal mol^{-1}). The solid-state configuration of **14** also suggests that the three *Si*-Me groups would be inequivalent in the absence of rotation around the W–$SiMe_3$ axis. Indeed, at –20 °C the $SiMe_3$ resonance begins to broaden, and upon further cooling to –80 °C resolves into three sharp singlets of equal intensity at δ 0.79, 0.68, and 0.41 (Figure 8). This appears to be the first reported example of hindered rotation of a $SiMe_3$ group in a metal complex.

The structural studies described above reveal W–Si bonds in **14** which are longer than in the other silyl hydride and bis(silyl) complexes. It would appear, therefore, that the combination of bulky $Si(t\text{-}Bu)_2H$ and $SiMe_3$ ligands in **14** yields the most sterically destabilized complex of the series. The W–$Si(t\text{-}Bu)_2H$ distance in silyl hydride **6b** is also long compared to the smaller silyls examined. It is, therefore, not surprising that **14** and **6a,b** exhibit variable temperature ^1H NMR spectra due to hindered rotation at the W–Si bonds. It is not immediately obvious, however, that the most sterically encumbered complex, **14**, should exhibit a barrier to rotation which is 7 kcal mol^{-1} *lower* than the apparently less-crowded **6**. Interestingly, a similar situation was observed in a series of tantalum silyl complexes, $Cp_2Ta(SiR_3)(L)$.[30] Structural studies and chemical reactivity patterns clearly indicate that $Cp_2Ta(Si(t\text{-}Bu)_2H)(PMe_3)$ is the most-hindered member of the series, yet the barrier to Ta–Si rotation in this complex is lower than in the carbonyl derivative $Cp_2Ta(Si(t\text{-}Bu)_2H)(CO)$, which is less labile and exhibits a substantially shorter Ta–Si bond distance. The pertinent values for $\Delta G^{\ddagger}_{rot}$ and M–Si bond distances for compounds **6a**, **6b**, **14**, and the two related tantalum compounds, $Cp_2Ta(PMe_3)(Si(t\text{-}Bu)_2H)$ and $Cp_2Ta(CO)(Si(t\text{-}Bu)_2H)$, are listed in Table 9.[30]

This apparent paradox is due to the fact that although the M–Si bond distances lengthen in response to increasing the overall steric congestion in the complexes, the height of the barrier to rotation around a M–SiR_3 bond reflects

---

(29) Mann, B. E.; Taylor, B. F. *^{13}C NMR Data for Organometallic Compounds*; Academic Press: London, 1981; p 38, 133.

(30) Jiang, Q.; Pestana, D. C.; Carroll, P. J.; Berry, D. H. *J. Am. Chem. Soc.*, submitted.

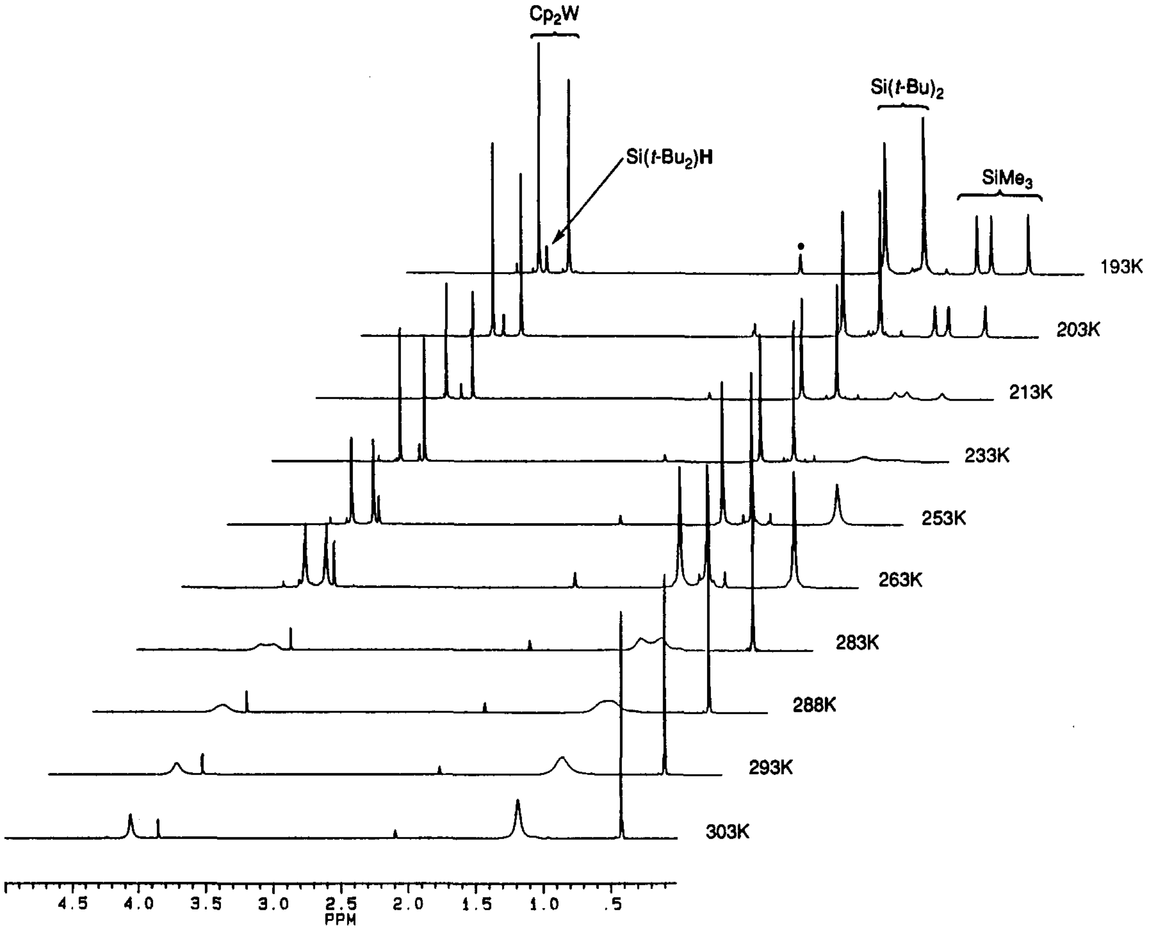

Figure 8. Variable-temperature ^{1}H NMR spectra (500 MHz) of **14** in toluene-d_8. Asterisk denotes residual protons in solvent.

a more specific interaction between the groups on silicon and the two Cp rings. In other words, the somewhat less-hindered complexes **6a,b** and the tantalum carbonyl permit a closer contact between the metal and the bulky silyl group than in **14** and the tantalum phosphine derivative, but this deeper penetration into the equatorial wedge locks the Si(*t*-Bu)$_2$H) group into a single rotational conformation. Interconversion of the conformers requires rotation of the M–Si(*t*-Bu)$_2$H) bond through a symmetrical transition state in which both *t*-butyl groups are thrust directly into the Cp rings. Ironically, this transition state is easier to achieve for the more-hindered complexes, because the entire silyl group is held further away from the Cp rings in the ground state. That **14** is a very sterically congested molecule is apparent from the fact the W–SiMe$_3$ bond rotation is hindered. In this case it is not only Cp–silyl interactions which lock the SiMe$_3$ group in place, but rather close contact with the adjacent (and hindered) Si(*t*-Bu)$_2$H group.

Experimental Section

General Considerations. All manipulations were carried out under dry nitrogen using high vacuum line or Schlenk techniques or a glove box under an atmosphere of prepurified N$_2$. Glassware was oven-dried before used. Petroleum ether (boiling range 35–65 °C), tetrahydrofuran (THF), dimethoxyethane (DME), benzene, and toluene were freshly distilled from sodium/benzophenone ketyl. Cp$_2$MoH$_2$ (**1**),[31] Cp$_2$WH$_2$ (**2**),[32] and Cp$_2$W(η^2-CH$_2$SiMe$_2$) (**10**)[3a] were prepared according to the literature methods. Chlorosilanes (Petrarch Systems, Inc.) were dried over 4-Å molecular sieves and degassed before use. Most organohydridosilanes were prepared by reduction of the appropriate chlorosilane with lithium aluminum hydride. (*t*-Bu)$_2$SiH$_2$ was obtained from Lithium Corp. of America. Photochemical reactions were carried out in a Rayonet Photochemical Reactor using low-pressure mercury arc lamps (350 nm). Routine ^{1}H NMR spectra were obtained using IBM Bruker AC 250 or AM 200 spectrometers. ^{13}C NMR experiments were performed on a IBM-Bruker AM 500 spectrometer using the DEPT or INEPT pulse sequences or gated coupled spectra to obtain coupling constants. ^{29}Si spectra were obtained at 40 MHz on a Bruker AF-200 spectrometer with a broad band multinuclear probe using the DEPT pulse sequence. Benzene-d_6 was used as NMR solvent unless otherwise indicated. The ^{1}H, ^{13}C, and ^{29}Si spectra were referenced to SiMe$_4$. Elemental analyses were performed by Desert Analytics, Galbraith, or Robertson Laboratories.

Preparation of Cp$_2$Mo(H)(SiMe$_2$H), 3. A solution of **1** (100 mg, 0.44 mmol) and Me$_2$SiH$_2$ (0.90 mmol) in 15 mL of benzene was photolyzed for 20 h at 40 °C. The volatiles were removed under vacuum. Sublimation at 70 °C and 10^{-3} Torr yielded 100 mg (0.35 mmol) of yellow product (79% yield).

Preparation of Cp$_2$Mo(H)(SiMe$_2$Cl), 4a. A solution of **1** (250 mg, 1.10 mmol) and Me$_2$Si(H)Cl (2.25 mmol) in 15 mL of benzene was photolyzed for 36 h at 40 °C. The volatiles were removed under vacuum. Sublimation at 70 °C and 10^{-3} Torr yielded 275 mg (0.86 mmol) of yellow product (78% yield). Anal. Calcd for C$_{12}$H$_{17}$ClMoSi: C, 44.94; H, 5.34. Found: C, 44.07; H, 5.52.

Preparation of Cp$_2$Mo(Cl)(SiMe$_2$Cl), 4b. A solution of **4a** (115 mg, 0.36 mmol) and CCl$_4$ (0.40 mmol) in 20 mL of benzene was stirred for 1.5 h at 25 °C. The volatiles were removed under vacuum yielding 96 mg (0.27 mmol) of burgundy product (75% yield).

---

(31) Silavwe, N. D.; Castellani, M. P.; Tyler, D. R. *Inorg. Synth.* **1992**, *29*, 204.

(32) (a) Cp$_2$WH$_2$ was synthesized by adapting the method described in ref 31 to tungsten. (b) A less labor-consuming prep has been recently reported for Cp$_2$WH$_2$: Persson, C.; Andersson, C. *Organometallics* **1993**, *12*, 2370.

Preparation of $Cp_2Mo(H)(SiMe_3)$, 5a. A solution of 1 (100 mg, 0.44 mmol) and Me_3SiH (1.00 mmol) in 15 mL of benzene was photolyzed for 46 h at 18 °C. The volatiles were removed under vacuum. Sublimation at 70 °C and 10^{-3} Torr yielded 120 mg (0.40 mmol) of yellow product (91%). Anal. Calcd for $C_{13}H_{20}MoSi$: C, 51.99; H, 6.71. Found: C, 51.64; H, 6.91.

Preparation of $Cp'_2Mo(H)(SiMe_3)$, 5b. A solution of Cp'_2MoH_2 (200 mg, 0.78 mmol) and Me_3SiH (1.6 mmol) in 15 mL of benzene was photolyzed for 36 h at 10 °C. The volatiles were removed under vacuum. Sublimation at 60 °C and 10^{-3} Torr yielded 250 mg (0.76 mmol) of yellow product (98% yield). Anal. Calcd for $C_{15}H_{24}MoSi$: C, 54.86; H, 7.37. Found: C, 54.91; H, 7.40.

Preparation of $Cp_2Mo(H)(Si(t\text{-}Bu)_2H)$, 6a. A solution of 1 (325 mg, 1.43 mmol) and 0.5 mL (2.78 mmol) $(t\text{-}Bu)_2SiH_2$ in 15 mL of benzene was photolyzed at 40 °C for 56 h. The volatiles were removed under vacuum. Excess silane was removed by trituration with petroleum ether. Sublimation at 50 °C and 10^{-3} Torr yielded 350 mg of yellow product (72% yield).

Preparation of $Cp'_2Mo(H)(Si(t\text{-}Bu)_2H)$, 6b. A solution of Cp'_2MoH_2 (150 mg, 0.58 mmol) and $(t\text{-}Bu)_2SiH_2$ (215 mg, 1.5 mmol) in 15 mL of toluene was photolyzed for 36 h at 10 °C. The volatiles were removed under vacuum. Sublimation at 65 °C and 10^{-3} Torr yielded 170 mg (0.43 mmol) of yellow product (74% yield). Anal. Calcd for $C_{20}H_{34}MoSi$: C, 60.28; H, 8.60. Found: C, 60.32; H, 8.20.

Preparation of $Cp_2Mo(H)(Si(t\text{-}Bu)_2Cl)$, 7. A solution of 1 (235 mg, 1.03 mmol) and $(t\text{-}Bu)_2Si(H)Cl$ (2.06 mmol) in 15 mL of toluene was photolyzed for 36 h at 10 °C. Volatiles were removed under vacuum and excess $(t\text{-}Bu)_2SiHCl$ was removed by trituration with petroleum ether. Sublimation at 70 °C and 10^{-3} Torr yielded 325 mg (0.80 mmol) of yellow product (78% yield).

Preparation of $Cp_2W(H)(SiMe_2Cl)$, 8. A solution of 2 (100 mg, 0.32 mmol) in neat Me_2SiHCl was photolyzed at 40 °C for 11 days with periodic freeze-pump-thaw cycles to remove liberated H_2. The volatiles were removed under vacuum. Sublimation at 70 °C and 10^{-3} Torr yielded 65 mg (0.16 mmol) of orange-yellow product (50% yield).

Preparation of $Cp_2W(H)(SiMe_3)$, 9. A solution of 2 (52 mg, 0.16 mmol) and Me_3SiH (1.65 mmol) in 5 mL of cyclohexane was photolyzed for 5 days with periodic freeze-pump-thaw cycles to remove liberated H_2. The volatiles were removed under vacuum. Sublimation at 70 °C and 10^{-3} Torr yielded 37 mg (0.01 mmol) of yellow product (60% yield). Anal. Calcd for $C_{13}H_{20}WSi$: C, 40.22; H, 5.19. Found: C, 39.85; H, 5.19.

Formation of $Cp_2W(H)(SiMe_3)$, 9. An NMR tube containing 5 mg (0.013 mmol) of 10 in 0.4 mL of benzene-d_6 was sealed under 3 atm of H_2 and the reaction monitored by ^1H NMR. After 10 days at 25 °C, the ^1H NMR showed quantitative conversion of **10** to **9**.

Preparation of $Cp_2W(SiMe_3)_2$, 11. To a benzene solution containing **10** (0.21 g, 0.54 mmol) was added $HSiMe_3$ (1.10 mmol). After stirring for 22 h at 25 °C, the volatiles were removed and the solids sublimed at 80 °C to yield 0.220 g (88%) of yellow compound. Recrystallization of the sublimate from toluene/hexanes yielded analytically pure crystals for elemental analysis. Anal. Calcd for $C_{16}H_{28}Si_{12}W$: C, 41.74; H, 61.3. Found: C, 41.87; H, 5.95.

Preparation of $Cp_2W(SiMe_3)(SiMe_2Cl)$, 12. To a toluene solution containing **10** (0.100 g, 0.26 mmol) was added $HSiMe_2Cl$ (0.906 g, 1.02 mmol). After stirring for 28 h at room temperature, the volatiles were removed and the solids recrystallized from toluene/hexanes to yield 0.105 g (84%) of yellow crystals. Anal. Calcd for $C_{15}H_{25}ClSi_2W$: C, 37.47; H, 5.24. Found: C, 37.36; H, 5.06.

Preparation of $Cp_2W(SiMe_3)(Si(i\text{-}Pr)_2Cl)$, 13. To a toluene solution containing **10** (0.100 g, 0.26 mmol) was added $HSi(i\text{-}Pr)_2Cl$ (0.070 g, 0.47 mmol). After stirring for 41 h at 25 °C, the volatiles were removed under vacuum. Trituration with *n*-pentane followed by recrystallization from methylcyclohexane yielded 0.115 g (83%) of yellow crystals. Anal. Calcd for $C_{19}H_{33}ClSi_2W$: C, 42.50; H, 6.19. Found: C, 42.73; H, 6.32.

Preparation of $Cp_2W(SiMe_3)(Si(t\text{-}Bu)_2H)$, 14. A solution of **10** (0.125 g, 0.32 mmol) in neat $H_2Si(t\text{-}Bu)_2$ (20 mL) was stirred at 65 °C for 47 h. The silane was removed under vacuum, and the solids were triturated with *n*-pentane. Recrystallization from *n*-pentane yielded 0.150 g (88%) of yellow crystals. Anal. Calcd for $C_{21}H_{38}Si_2W$: C, 47.54; H, 7.22. Found: C, 47.25; H, 7.19.

Structure Determinations of 3, 4, 5b, 6b, 9, 13, and 14. Single crystals of suitable size were grown from toluene/hexanes at −35 °C and sealed in 0.5-mm thin-walled Pyrex capillaries in the glovebox, and the capillaries were mounted on the diffractometer. Refined cell dimensions and their standard deviations were obtained from least-squares refinement of 25 accurately centered reflections with $2\theta > 25°$. Crystal data are summarized in Tables 3 and 4.

Diffraction data were collected at 295 K on an Enraf-Nonius four-circle CAD-4 diffractometer employing Mo Kα radiation filtered through a highly oriented graphite crystal monochromator. The intensities of three standard reflections measured at intervals of ca. 80 reflections showed no systematic change during the data collections. Data collections are summarized in Tables 3 and 4. The raw intensities were corrected for Lorentz and polarization effects by use of the program BEGIN from the SDP+ packages.[33] Empirical absorption corrections based on ψ scans were also applied where indicated.

All calculations were performed on a VAX 11/785 computer with the SDP+ software package.[33] The full-matrix least-squares refinement was based on F, and the function minimized was $\sum w(|F_o|-|F_c|)^2$. The weights (w) were taken as $4F_o^2/(\sigma(F_o^2))^2$ where $|F_o|$ and $|F_c|$ are the observed and calculated structure factor amplitudes. Atomic scattering factors were taken from ref 34. Agreement factors are defined as $R_1 = \sum||F_o| - |F_c||/\sum|F_o|$ and $R_2 = [\sum w||F_o| - |F_c||^2/\sum w|F_o|^2]^{1/2}$. The goodness of fit is defined as GOF = $[\sum w(|F_o| - |F_c|)^2/(N_o - N_p)]^{1/2}$, where N_o and N_p are the numbers of observations and parameters.

The coordinates of the metal and silicon atoms were obtained from three-dimensional Patterson Maps. Analysis of subsequent difference Fourier maps led to the location of the remaining heavy atoms. Refinements using anisotropic Gaussian amplitudes followed by difference Fourier synthesis resulted in the location of most of the Cp hydrogens and at least one hydrogen in each methyl group. The positions of all hydrogens on carbon were optimized (D(C–H) = 0.95 Å) using of the program HYDRO.[33] The positions of the silicon and molybdenum hydrides in **3**, **4a**, **5b**, and **6b** were located from electron density maps and were successfully refined with isotropic thermal parmeters. The position of the silicon hydride in **14** was located and refined using a fixed isotropic thermal parameter. The tungsten hydride in **9** was not located. Final refinement included anisotropic thermal parameters for all non-hydrogen atoms. Final positional parameters, thermal parameters, and complete tables of bond distances and angles for all the structures are included in the supplementary material.

Acknowledgment. Financial support of this work by the National Science Foundation (Grant No. CHE-9014625) and Petroleum Research Fund (Grant No. 22546-AC3) is gratefully acknowledged. We also thank Terry Rathman of Lithco for a generous gift of $(t\text{-}Bu)_2SiH_2$.

Supplementary Material Available: Tables of positional and thermal parameters and bond distances and angles for **3**, **4a**, **5b**, **6b**, **9**, **13**, and **14** (45 pages). Ordering information is given on any current masthead page.

OM930685U

---

(33) B. A. Frenz and Associates, Inc., College Station, TX 77840, and Enraf-Nonius, Delft, Holland.

(34) *International Tables for X-Ray Crystallography*; Kynoch: Birmingham, England, 1974; Vol. IV.